lubricants

MDPI

Article

Eco-Friendly Water-Based Nanolubricants for Industrial-Scale Hot Steel Rolling

Hui Wu [1], Hamidreza Kamali [1], Mingshuai Huo [1], Fei Lin [1], Shuiquan Huang [2], Han Huang [2], Sihai Jiao [3], Zhao Xing [3] and Zhengyi Jiang [1,*]

[1] School of Mechanical, Materials, Mechatronic and Biomedical Engineering, University of Wollongong, Wollongong, NSW 2522, Australia; hwu@uow.edu.au (H.W.); hk207@uowmail.edu.au (H.K.); mh317@uowmail.edu.au (M.H.); fl236@uowmail.edu.au (F.L.)

[2] School of Mechanical and Mining Engineering, The University of Queensland, Brisbane, QLD 4072, Australia; shuiquan.huang@uq.edu.au (S.H.); han.huang@uq.edu.au (H.H.)

[3] Baosteel Research Institute (R&D Centre), Baoshan Iron & Steel Co., Ltd., Shanghai 200431, China; shjiao@baosteel.com (S.J.); xingzhao@baosteel.com (Z.X.)

* Correspondence: jiang@uow.edu.au

Received: 30 September 2020; Accepted: 23 October 2020; Published: 27 October 2020

Abstract: Eco-friendly and low-cost water-based nanolubricants containing rutile TiO_2 nanoparticles (NPs) were developed for accelerating their applications in industrial-scale hot steel rolling. The lubrication performance of developed nanolubricants was evaluated in a 2-high Hille 100 experimental rolling mill at a rolling temperature of 850 °C in comparison to that of pure water. The results indicate that the use of nanolubricant enables one to decrease the rolling force, reduce the surface roughness and the oxide scale thickness, and enhance the surface hardness. In particular, the nanolubricant consisting of 4 wt % TiO_2, 10 wt % glycerol, 0.2 wt % sodium dodecyl benzene sulfonate (SDBS) and 1 wt % Snailcool exhibits the best lubrication performance by lowering the rolling force, surface roughness and oxide scale thickness by up to 8.1%, 53.7% and 50%, respectively. The surface hardness is increased by 4.4%. The corresponding lubrication mechanisms are attributed to its superior wettability and thermal conductivity associated with the synergistic effect of rolling, mending and laminae forming that are contributed by TiO_2 NPs.

Keywords: eco-friendly; water-based nanolubricant; industrial-scale; hot rolling

1. Introduction

Hot-rolled steels have been extensively used in the modern manufacturing industry as either an end product or a raw material for subsequent processing. In practical hot rolling, steel slabs are normally reheated to 1150–1250 °C, followed by continuous plastic deformation until the finishing rolling temperature achieves around 800 °C [1]. Because of such a high temperature of the steel and the friction between the work roll and the steel workpiece, a coolant and/or a lubricant is required in each rolling mill [2]. In recent decades, considerable studies have been focused on using neat oils and oil-in-water emulsions as representative lubricants in hot rolling to obtain reduced rolling force and roll wear [3,4], thinned oxide scale [5], improved surface quality [6], controlled profile and flatness [7], even refined grains and optimised texture [8–10]. In view of the above, the energy consumption of the rolling mill can thus be decreased, and meanwhile rolling high-strength steels can be readily realised within the limits of mill load. Besides, it enables reduced roll changing frequency and increased productivity. More importantly, the yield and overall quality and properties of rolled products are therefore greatly enhanced. However, the use of oil-containing lubricants inevitably brings forth environmental pollution when burned and discharged, and regular maintenance of oil

nozzles is always a demanding job. In light of this, it is imperative to use eco-friendly lubricants as alternatives to the oil-containing ones for environmental purpose. One of the most promising candidates is water-based nanolubricant.

It is well-known that water is not only a clean and low-cost lubricant, but also an excellent coolant due to its high specific heat capacity. Nevertheless, its corrosive properties and poor viscosity restrain it from being used in most engineering applications. In order to improve the lubrication performance of water, recent research has been devoted to using various nanomaterials as nanoadditives dispersed in water [11–16]. These nanoadditives contribute to enhancing friction-reduction, anti-wear and load-carrying capacities of base water to a large extent, which shows great potential to be applied in hot steel rolling. To name a few, He et al. [17] added MoS_2-Al_2O_3 nanocomposite into water-based fluid for hot rolling in a 2-high rolling mill. They found that the rolling force and oxide scale thickness of rolled strips obtained using base-fluid lubricating condition were, respectively, reduced by 26.9% and 54.2% after 5-pass rolling. Meng et al. [18] used water-based anatase nano-TiO_2 lubricating fluid in a 4-high rolling mill. The results indicated that the grain size of rolled steel and the thickness of oxide scale were decreased by 60% and 17%, respectively, after 5-pass rolling, compared with those obtained without lubricant. Bao et al. [19] chose nano-SiO_2 as water-based lubricant additive and studied its effect on surface qualities of hot rolled strips. It was concluded that the use of 0.3 wt % SiO_2 lubricant resulted in improved surface topography, thinned oxide scale and refined surface microstructure. In particular, an increasing number of research efforts have been directed towards using TiO_2 nanoparticles (NPs) to synthesise eco-friendly water-based nanolubricants in different application areas. Table 1 provides a summary of some investigations that are related to the eco-friendly lubricants containing TiO_2 NPs. It can be seen that most of the TiO_2 NPs used in the lubricants have a particle size below 100 nm, and some are even smaller than 50 nm. This will cause a very high material cost. In addition, the dispersants are generally composted of complex chemical agents, and the synthesis of the lubricants always involves complicated processes, such as ultrasonic treatment. These are the disadvantages of achieving the industrial-scale application.

Table 1. Summary of eco-friendly water-based nanolubricants using TiO_2 nanoparticles (NPs).

Authors	NP Phase	NP Size	Dispersants	Application
Meng et al. [18]	Anatase	90 nm	Glycerin, Triethanolamine (TEA), Sodium polyacrylate (PAAS), Sodium hexametaphosphate (SHMP) etc.	Hot rolling
Kong et al. [20]	Anatase	20 nm	PAAS, SHMP	Tribology
Najiha et al. [21]	N/A	40 nm	Confidential	End milling
Ohenoja et al. [22]	Rutile	200 nm	PAAS	Grinding
Gu et al. [23]	Anatase	20 nm	Silane coupling agent, OP-10	Drilling

In our previous studies, the physicochemical and tribological properties of water-based nanolubricants containing P25 TiO_2 NPs were systematically investigated in terms of different loads, steel surfaces and temperatures [24–26]. The formulas of as-prepared water-based nanolubricants have been optimised, and therefore they exhibited largely enhanced lubrication performance in hot steel rolling [27–30]. However, all the fundamental research on water-based nanolubricants is only confined to the laboratory scale. Their applications in practical hot steel rolling are still restricted due to the high cost of nanomaterials being used.

For the purpose of accelerating the application and popularisation of water-based nanolubricant in industrial-scale hot steel rolling, relatively coarse, very low cost TiO_2 NPs were adopted in the present study. To compensate the degradation of dispersion stability and lubrication performance caused by coarsened nano-TiO_2, novel dispersant and extreme pressure agent were also added into the base water. The lubrication performance of newly developed eco-friendly water-based lubricants was characterised, and corresponding lubrication mechanisms were proposed in this study.

2. Materials and Experimental Procedure

2.1. Materials

Eco-friendly water-based nanolubricants being applied in this study consist of low-cost rutile TiO_2 NPs (~300 nm in diameter), glycerol, sodium dodecyl benzene sulfonate (SDBS) and snailcool. Rutile is the most stable polymorph of TiO_2 at all temperatures up to its melting point at 1843 °C, which can be irreversibly converted from metastable phases of anatase or brookite upon being heated above temperatures in the range of 600–800 °C [31,32]. Glycerol is a colorless, odorless and viscous liquid that aids in enhancing the viscosity and wettability of nanolubricants [28]. SDBS is an organic dispersant with a linear structure (LAS) and hydrophilic group, which helps improve the wettability, dispersion stability and also the viscosity of the nanolubricants [30]. Snailcool is a novel aqueous additive that not only boosts the extreme pressure property of the nanolubricants but also compensates the degradation of lubrication performance due to the use of relatively coarse TiO_2 NPs. All the additives are nontoxic chemicals and have strong biological degradability in the environment. The synthesis of the water-based nanolubricants is a facile process which only involves mechanical stirring without ultrasonic treatment. This is to further reduce the integrated cost of applying the water-based nanolubricants on an industrial scale. The formulation of as-synthesised nanolubricants in this study is based on the optimal TiO_2 concentrations obtained previously [27,30], and their chemical compositions are listed in Table 2. For comparison purpose, pure water, a commonly used coolant of industrial-scale work rolls, was selected as a benchmark. It is estimated that the cost of the as-synthesised water-based nanolubricant is less than USD 0.3/kg, which exhibits great potential in the industrial-scale hot steel rolling.

Table 2. Chemical compositions of applied lubricants.

Lubrication Type	Description
W	Water
A	2 wt % TiO_2 + 0.1 wt % SDBS + 1 wt % Snailcool
B	2 wt % TiO_2 + 0.2 wt % SDBS + 1 wt % Snailcool
C	2 wt % TiO_2 + 10 wt % glycerol + 0.2 wt % SDBS + 1 wt % Snailcool
D	4 wt % TiO_2 + 0.2 wt % SDBS + 1 wt % Snailcool
E	4 wt % TiO_2 + 10 wt % glycerol + 0.2 wt % SDBS + 1 wt % Snailcool

A mild steel with a yield stress of 345 MPa (namely Q345) was used in hot rolling. The main chemical compositions of steel Q345 in weight percentage are as follows: C 0.16%, Si 0.25%, Mn 1.5%, Mo 0.007%, Ni 0.006%, Cr 0.02% and Nb + V + Ti < 0.02%. The steel workpieces were machined to dimensions of 300 mm (Length) × 100 mm (Width) × 12 mm (Thickness) with tapered edges for an easy roll bite, as schematically shown in Figure 1. Both sides of the workpieces were ground to generate consistent surface roughness (R_a) of around 0.5 μm. Ahead of each hot rolling test, the workpiece was cleaned with acetone to remove any residues retained from machining.

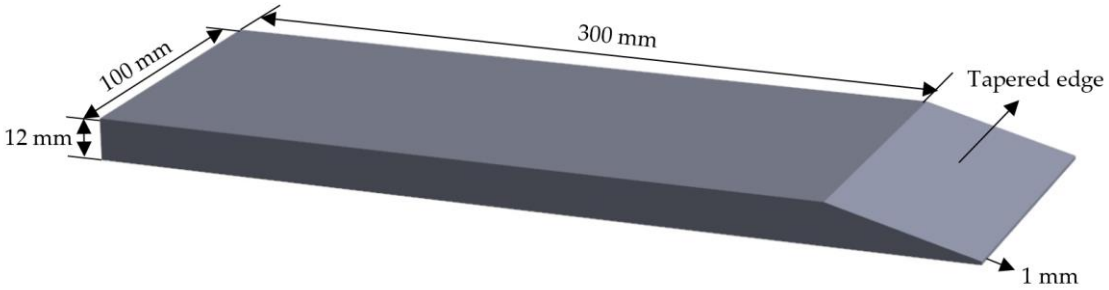

Figure 1. Schematic view of steel workpiece used for hot rolling.

2.2. Hot Rolling Test

The Q345 workpieces were hot rolled on a 2-high Hille 100 (Hille Engineering Company, Ltd., Sheffield, England) experimental rolling mill that was equipped with two work rolls with a dimension of Φ 225 mm × 254 mm and a surface roughness of 0.9 μm in R_a. During testing, the Q345 workpieces were heated in a high-temperature electric resistance furnace at 900 °C and soaked for 30 min in nitrogen atmosphere. The hot workpieces were then rolled at a temperature in the vicinity of 850 °C with a reduction of 26.9% and a rolling speed of 0.35 m/s under different lubrication conditions. After that, the rolled steels were immediately transferred into a cooling box filled with nitrogen. It is noted that the nitrogen being used in both the furnace and the cooling box was to eliminate the effect of oxide scale on the lubrication performance of applied lubricants and also minimise additional steel oxidation in air. By doing this, the initial rolling conditions would be easily controlled, and the study of oxide scale formation was primarily focused on the rolling process. As described somewhere [27], all the lubricants were continuously sprayed onto the pre-cleaned work roll surfaces before rolling until supersaturated adhesion was achieved. Hot steel rolling under the same testing condition was repeated three times to attain average data, including the rolling force, surface roughness and hardness of rolled steels, and the thickness of the oxide scale.

2.3. Characterisation Methods

The phase and morphology of the rutile TiO_2 NPs were characterised using an X-ray diffractometer (XRD, GBC Scientific Equipment Pty Ltd., Melbourne, Australia) and a high-resolution field emission scanning electron microscope (FESEM, JEOL Ltd., Tokyo, Japan).

The dispersion stability of prepared water-based nanolubricants was evaluated using sedimentation method for a direct observation of NP sediment, which was acquired by photo capturing within 48 h.

The rolling force data during hot rolling was recorded through two individual load cells located at both the drive and operation sides in the rolling mill. The data acquisition was performed by MATLAB xPC technology (2017b) (The MathWorks Inc., Natick, MA, USA).

The surface roughness and profile of rolled steels were obtained using a KEYENCE VK-X100K three-dimensional (3D) Laser Scanning Microscope (Keyence Corporation, Osaka, Japan). To ensure the measurement accuracy, five different spots along the rolling direction were selected, and then the data were averaged.

The cross sections of rolled steels along the rolling direction were observed under the 3D Laser Scanning Microscope to measure the oxide scale thickness. Prior to the observations, epoxy resin was mounted onto each surface of rolled steel followed by a dry cutting, grinding and polishing.

The surface microstructure of rolled steels was observed under the 3D Laser Scanning Microscope, and the hardness of surface substrate was measured using a Micro Vickers Hardness Tester (TIME GROUP INC., Beijing, China). To minimise data scattering, five different spots on each steel substrate were chosen for averaged values.

The wettability of the lubricants was evaluated by the measurement of contact angles on the surface of a roll material (High-Speed Steel, abbreviated as HSS) using a Rame-hart 290 Goniometer (Rame-hart instrument co., Succasunna, NJ, USA). Each measurement was repeated five times to obtain an average value.

The thermal conductivity of applied lubricants was measured at room temperature using a TCi Thermal Conductivity Analyzer (C-Therm Technologies Ltd., Fredericton, NB, Canada). Five measurements were conducted for each lubricant to ensure repeatability.

The surface and resin/oxide scale interface of the rolled steel were observed and analysed under the FESEM equipped with an energy-dispersive spectrometer (EDS, JEOL Ltd., Tokyo, Japan) to examine the lubrication mechanisms.

3. Results

3.1. Characterisation of Nanolubricant

Figure 2a shows the XRD pattern of the TiO_2 NPs being used in this study, suggesting a high-purity rutile by referring to the XRD standard atlas (JCPDS No. 21-1276). As can be seen from Figure 2b, the rutile TiO_2 NPs are nearly spherical with an average size of approximately 300 nm. It is expected that the small size difference provides an effective assurance for consistent lubrication performance in a stable industrial-scale hot steel rolling.

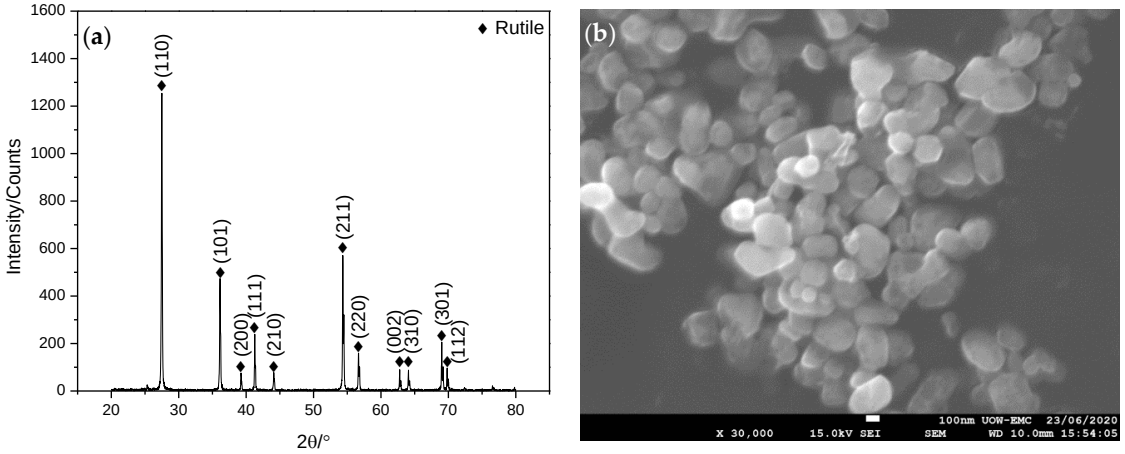

Figure 2. (**a**) X-ray diffractometer (XRD) pattern and (**b**) scanning electron microscope (SEM) image of TiO_2 NPs.

Figure 3 shows the sedimentation of TiO_2 NPs in different water-based nanolubricants at varying settling times. Regardless of the composition, it can be found that as-synthesised suspensions remain stable without apparent particle sedimentation within 120 min. Even after standing the suspensions for 24 h, the TiO_2 NPs settle down slightly, and a shallow supernatant appears. This phenomenon reveals excellent dispersion stability of the water-based nanolubricants, which are hence applicably supplied in the industrial-scale hot steel rolling with the considerations of their stable periods and the roll changing frequency.

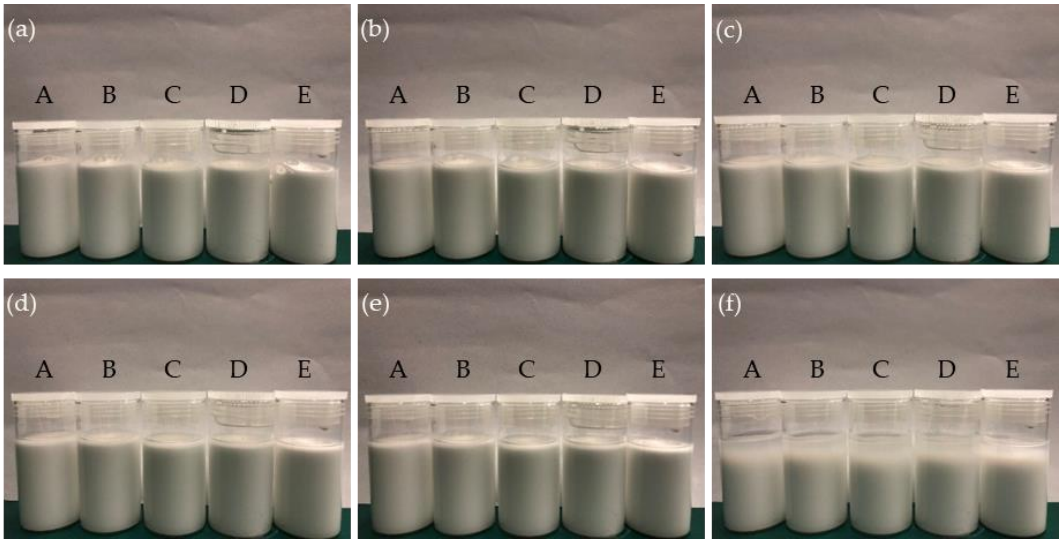

Figure 3. Sedimentation of TiO_2 NPs dispersed in different water-based nanolubricants at a settling time of (**a**) 0; (**b**) 30 min; (**c**) 60 min; (**d**) 90 min; (**e**) 120 min; and (**f**) 48 h.

3.2. Rolling Force

Figure 4 shows the rolling force data obtained at a rolling temperature of 850 °C using water (benchmark) and different water-based nanolubricants. It is evident that the use of water results in the highest rolling force value (637.9 KN) among all the lubricants. In comparison to the case of water, the use of lubricant A slightly decreases the rolling force by only 1.5%. An increase in SDBS concentration in lubricant B enables a further decrease in rolling force but to a limited extent. However, the addition of glycerol in lubricant C helps significantly decrease the rolling force of water by around 5.4%, suggesting an important role of glycerol in the lubricant formulation. Compared to lubricant B, the increase in nano-TiO_2 concentration in lubricant D has a much better effect on decreasing the rolling force. In particular, lubricant D is still superior to lubricant C in spite of its lack of glycerol. Given the advantages of increased concentrations of TiO_2 NPs, glycerol and SDBS, the lowest rolling force value (586.2 KN) can be achieved when using lubricant E, which is 8.1% lower than that of water.

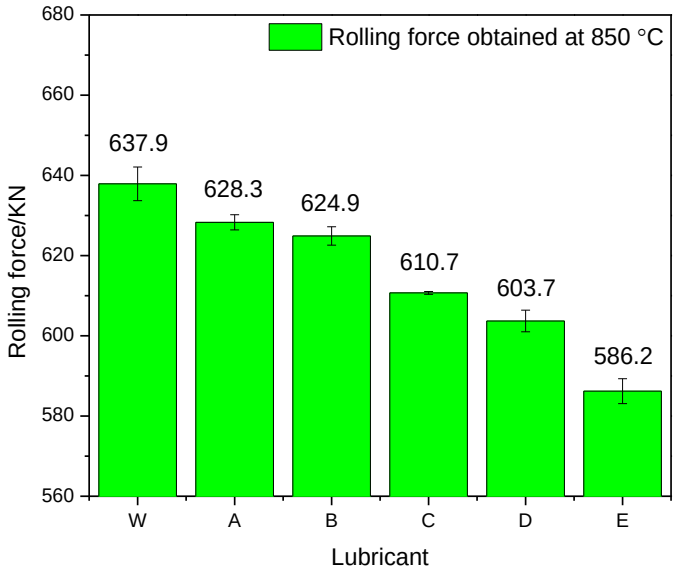

Figure 4. Rolling force obtained at 850 °C under different lubrication conditions.

3.3. Surface Morphologies

Figure 5 displays the 3D surface morphologies of rolled steels using the same lubrication conditions to those in Figure 4. It can be seen from Figure 5a that there are considerable humps and hollows throughout the surface under water lubrication, which presents the roughest surface condition among all the surfaces being generated. In contrast, the use of lubricant A remarkably flattens the surface with decreased peaks and valleys (see Figure 5b). Additionally, the surface becomes increasingly smooth by means of lubricants B, C and D, successively (see Figure 3c–e). It is noted that the smoothest surface is attained using lubricant E, indicating minimum surface undulations (see Figure 5f). By referring to these 3D morphologies, the surface roughness of rolled steels is quantified in Figure 6. It is concluded that the varying trend of the surface roughness is consistent with that of the rolling force. Likewise, the best lubrication effect is achieved when using lubricant E, which leads to over 50% lower surface roughness than that of water.

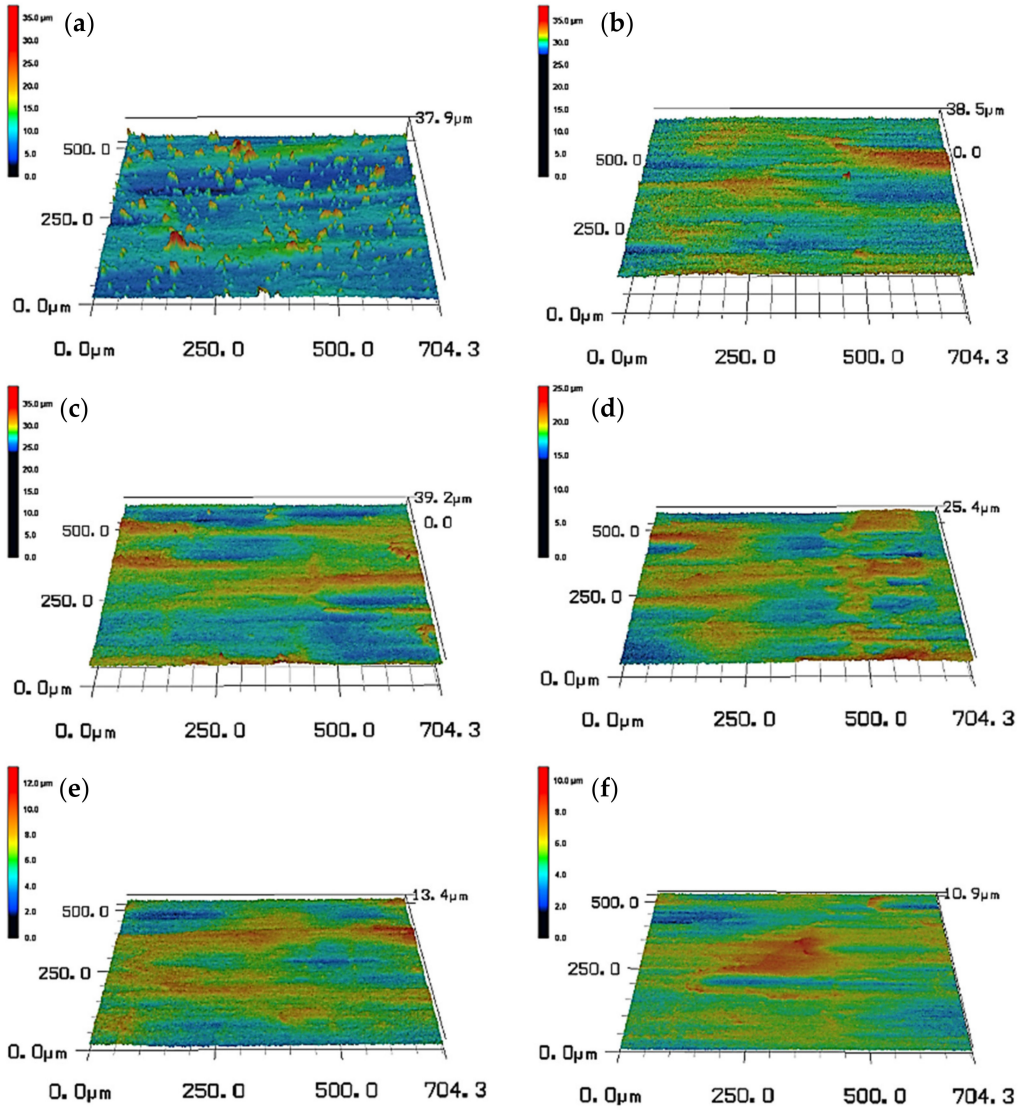

Figure 5. Three-dimensional surface morphologies of rolled steels at 850 °C under different lubrication conditions of (**a**) water; (**b**) lubricant A; (**c**) lubricant B; (**d**) lubricant C; (**e**) lubricant D; and (**f**) lubricant E.

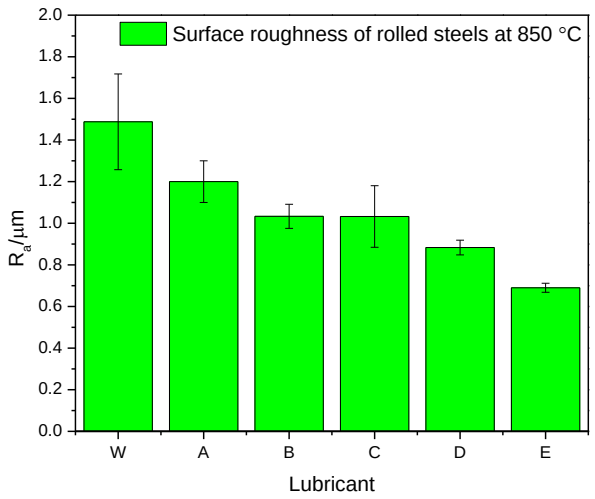

Figure 6. Surface roughness of rolled steels at 850 °C under different lubrication conditions.

3.4. Thickness of Oxide Scale

Figure 7 shows the optimal images of a cross section of oxide scales formed under some selected lubrication conditions. It is found in Figure 7a that rolling with pure water induces the thickest oxide scale among all the cases. Considerable pores and cracks can also be found inside the oxide scale. For the steel rolled with lubricant B, by comparison, less pores and almost no cracks are produced in the oxide scale, and its thickness becomes relatively thinner (see Figure 7b). The scale thickness is further decreased progressively, and the decrease reaches the maximum when using lubricant E (see Figure 7c). Meanwhile, the oxide scale becomes compact, and few pores can be seen in the oxide scale. According to quantitative comparison, the oxide scale formed under pure water condition is maximally thinned by up to 50% by the use of lubricant E.

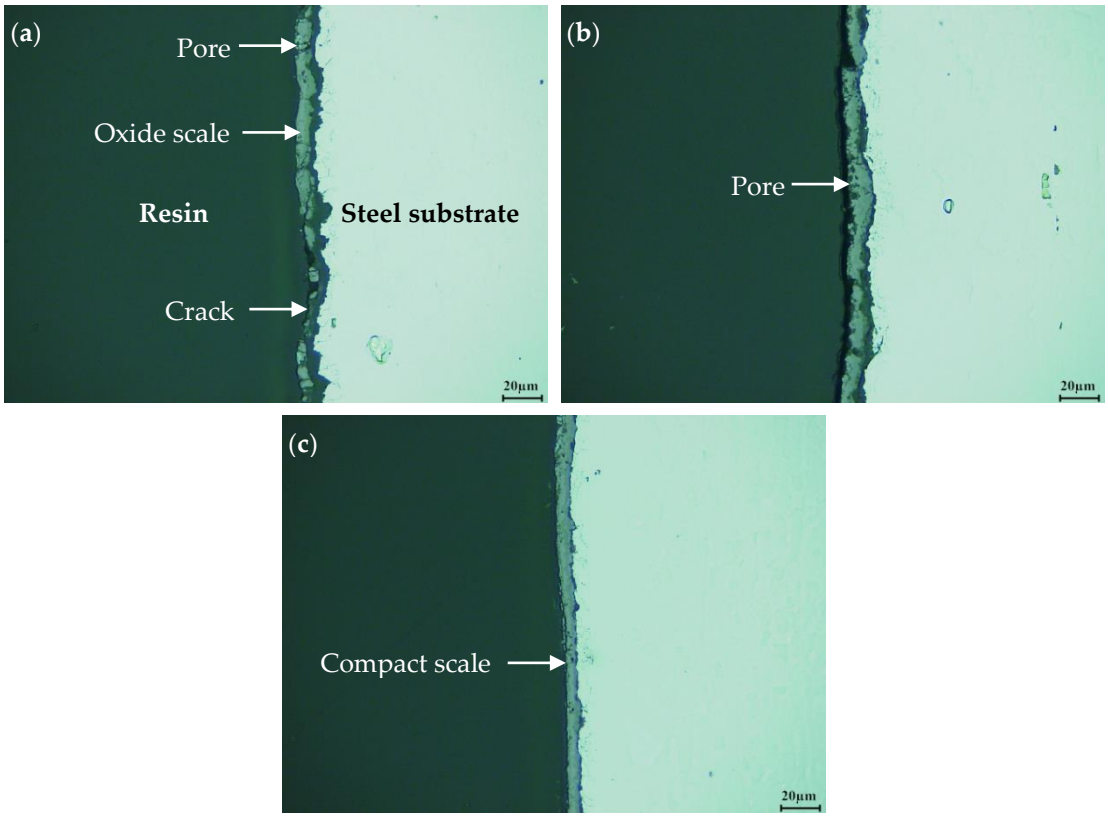

Figure 7. Optimal images of the cross section of oxide scales formed under different lubrication conditions of (**a**) water; (**b**) lubricant B; and (**c**) lubricant E.

3.5. Surface Microstructure and Hardness

Some selected surface microstructures of steels rolled with water, lubricants C and E are presented in Figure 8a, b, and c, respectively. It can be seen that the steel is composed of the majority of ferrite and a small amount of pearlite after rolling with water. The proportion of pearlite increases with the use of lubricant C, and it tends to reach the maximum after rolling with lubricant E. The grain size of ferrite, however, is not changed significantly, regardless of the lubricant being used. The surface hardness of rolled steels varying with different lubricants is shown in Figure 8d. This figure demonstrates that the surface hardness is inclined to increase with the use of nanolubricants until it achieves the highest value (136.2 HV) under lubricant E, suggesting a 4.4% rise in comparison to that of water.

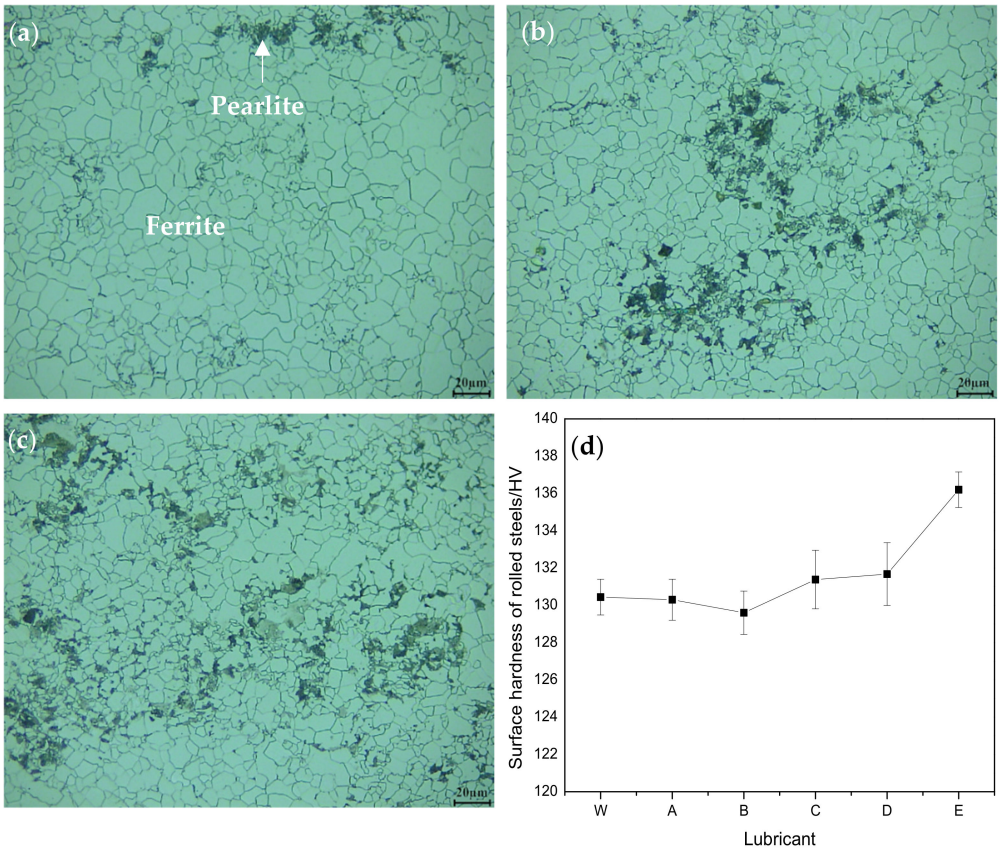

Figure 8. Surface microstructures of rolled steels using (**a**) water; (**b**) lubricant C and (**c**) lubricant E; and (**d**) surface hardness as a function of various lubricants.

4. Discussion

4.1. Wettability and Thermal Conductivity

As reported somewhere, appropriate wettability is a prerequisite to form effective and adhesive lubricating film on a metal surface where a friction pair can be restricted from direct contact [11,33]. Wettability is generally evaluated by the magnitude of contact angle (CA), and a smaller CA implies better wettability [34]. The CA values measured on a HSS surface using various lubricants and corresponding images of micro droplets are compared in Figure 9a. It reveals that pure water induces the largest CA (74.1°), suggesting the worst wettability among all lubricants. By contrast, lubricant A enables a significant drop in CA (42.4°), which tends towards a continuously slight decline with the use of lubricants B, C and D, successively. Most obviously, the lowest CA (36.7°) is attained by the use of lubricant E, which indicates the best wettability instead. By comparing the different compositions in various lubricants, it can be thus concluded that the addition of glycerol and SDBS is conducive to the improvement of wettability, which becomes particularly remarkable when there is an increase in TiO_2 concentration. These findings have been well explained and consistent with those in our previous study [30], although the particle size of nano-TiO_2 used in this study is relatively larger. It needs to be emphasised that the lubricant with better wettability on work roll surfaces is more likely to accommodate effective amounts of TiO_2 NPs and other additives which can be transferred to the contact zone between the work roll and the workpiece. The friction in the contact zone is thus reduced, and thereby the rolling force is decreased.

Thermal conductivity (TC) of the nanolubricants is an essential thermophysical property that determines their heat transfer ability when being used in hot steel rolling. The TC measured using various lubricants is shown in Figure 9b. It can be found that water has the lowest TC value (0.6 W/mK) among all the lubricants at an ambient temperature of 23 °C. Nevertheless, the water-based

nanolubricants being used all exhibit much higher TC than that of water. The changes in TC between lubricants B and D together with those between lubricants C and E both indicate that the increase in nano-TiO_2 concentration facilitates the increase in TC, which has good agreements with the results obtained elsewhere [35–37]. Besides, the TC of nanolubricants in this study is almost three times higher than that (~0.57 W/mK) in our previous study where TiO_2 NPs with 20 nm in diameter has been used. This huge difference is primarily ascribed to the substantiation that TC increases with increasing NP size [38]. However, the addition of glycerol in lubricant is detrimental to the increase in TC due to its intrinsic very low TC value (0.29 W/mK) [39]. In spite of this, the actually effective heat transfer ability, i.e., cooling rate, does not only consist in TC, but also in wettability (see Figure 9a), since the latter determines the amount of lubricants adhered onto the work roll surfaces. Consequently, the nanolubricants serve as better coolants than pure water on both work roll and workpiece surfaces, and their cooling rates increase with the increase in wettability while the TC changes insignificantly. Even though all the lubricants experienced a high temperature in the contact zone, the comparison of TC at ambient temperature is still applicable at such high temperatures, as TC increases with temperature elevation [40,41]. Accordingly, relatively more pearlite is transformed from austenite and retained in the microstructure, owing to a higher cooling rate [42]. As pearlite is harder than ferrite, this will lead to increased Vickers hardness on the surface of rolled steel (see Figure 8).

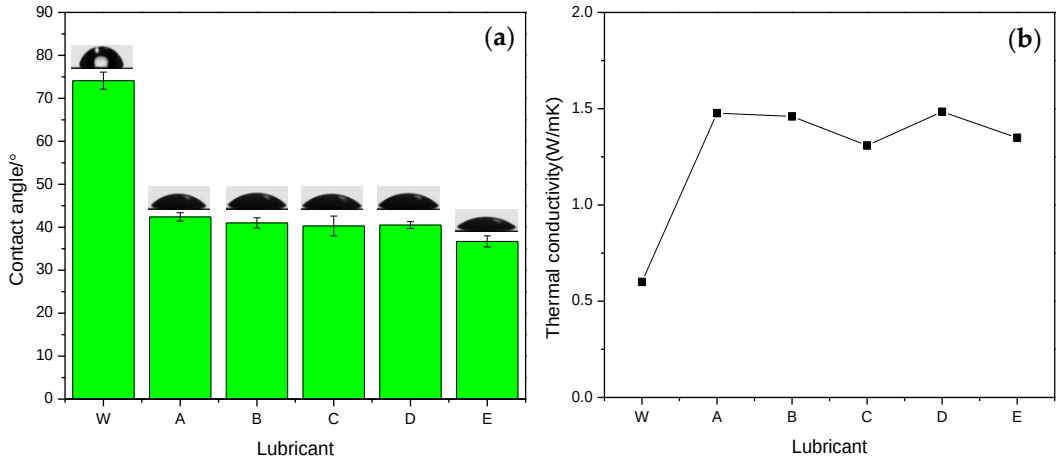

Figure 9. (**a**) Contact angle values measured on a High-Speed Steel (HSS) surface and (**b**) thermal conductivity measured at ambient temperature using various lubricants.

4.2. Analyses of Surface and Resin/Oxide Scale Interface

Figure 10a shows the SEM image of the rolled steel surface under water lubrication. It is apparently observed that the use of water brings forth substantial pores and cracks which spread over the surface. This phenomenon coincides with that shown in Figure 7a. To explain this, it is important to note that the oxidation of steel in this study experienced a varying temperature range and atmospheres, starting from heating in the furnace with nitrogen, transient cooling during the rolling process in air, and final cooling in the box filled with nitrogen. Thermal stress will be generated in the continuous cooling, as the thermal expansion coefficient changes in different oxide layers [43]. The presence of thermal stress is the main reason to produce pores and cracks inside the scale. In particular, the highest rolling force obtained by rolling with water is another reason to accelerate the propagation of pores and cracks. It is thus easy to understand that the compact surface produced in Figure 10b may be ascribed to the lowest rolling force achieved when rolling with lubricant E. Other possible reasons will be discussed later through the EDS mappings on the surface and the cross section. In order to further examine and compare the formation of oxide scale under water and lubricant E, the XRD patterns of the scale surface are shown in Figure 10c,d. All the peaks are indexed according to JCPDS cards Nos. 87-1166, 89-0688, 74-1886 and 89-7194 for Fe_2O_3, Fe_3O_4, FeO and Fe, respectively. It is clearly

observed that the peaks of Fe at 44.67° and 65.02° are weakened significantly on the surface lubricated by lubricant E, which corresponds to largely decreased pores and cracks (see Figure 10b). Instead, the peak intensities of FeO at 41.57° and 60.25° are strengthened after using lubricant E, indicating that more FeO has been retained. It is generally acknowledged that the diffusions of both iron and oxygen ions in opposite direction are supposed to trigger the formation of a tertiary oxide layer consisting of FeO, Fe_3O_4 and Fe_2O_3 on an iron surface above 570 °C from the innermost layer to the outmost [44]. For the steel experiencing hot rolling, the conversions of FeO to Fe_3O_4 and Fe_3O_4 to Fe_2O_3 commence from the surfaces of FeO and Fe_3O_4 where pores and cracks exist [29]. These pores and cracks provide abundant channels for oxygen penetration, which promotes aforementioned conversions and growth of oxide scale. Therefore, less FeO remains and thicker oxide scale is formed under water lubrication, compared to those that occurred under lubricant E. It is worth noting that the decomposition of FeO to Fe_3O_4 is the dominant conversion once the steel is cooled to the temperature below 570 °C [45]. This conversion together with those occurred above 570 °C will affect the main phase compositions in the oxide scale, leading to different intensities of Fe_3O_4 and Fe_2O_3, as shown in Figure 10c,d.

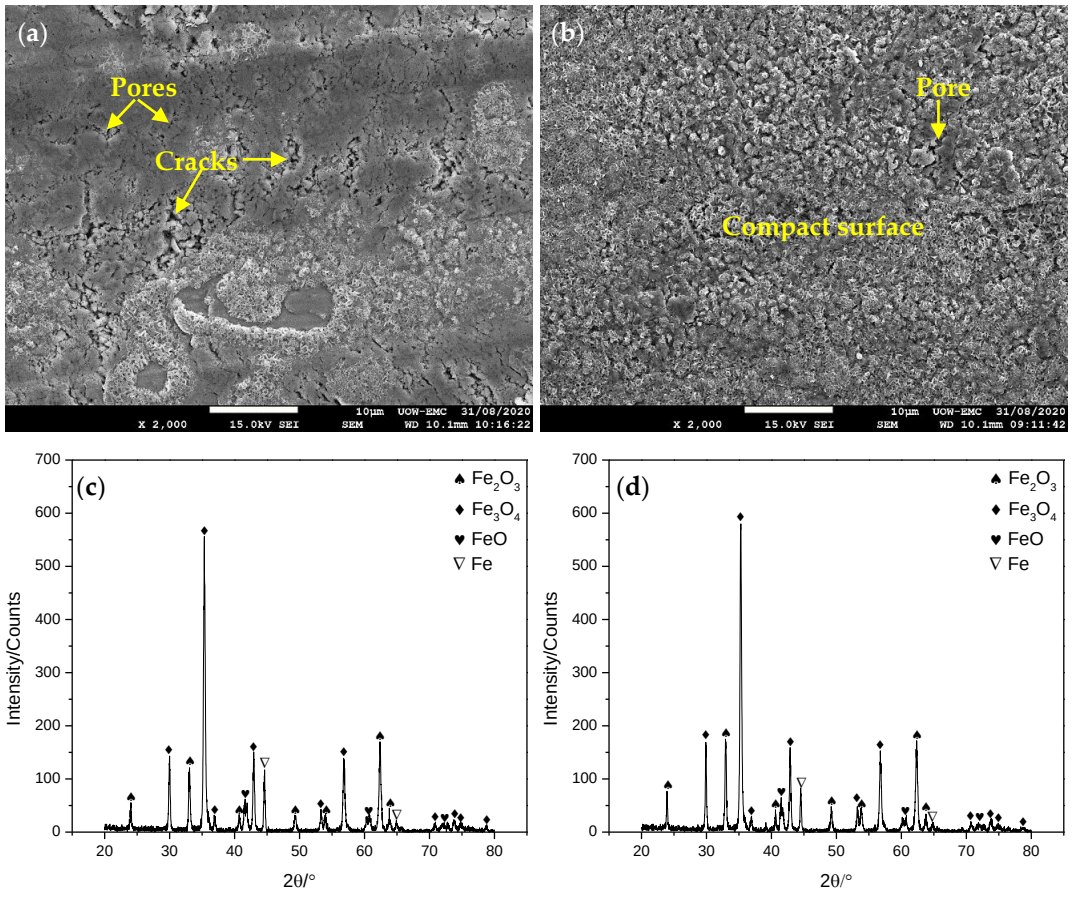

Figure 10. SEM images and XRD patterns of the steel surfaces rolled with (**a**,**c**) water and (**b**,**d**) lubricant E.

Figure 11 shows the SEM images and EDS mappings of the rolled steel surfaces observed under different magnifications using lubricant E. The EDS mappings of Ti and O in Figure 11a reveal the presence of well-distributed TiO_2 NPs and clusters. These typical morphologies are magnified in Figure 11b. Taking into account specific features in the SEM image and corresponding EDS mappings, it can be seen that TiO_2 NPs are able to fill in the surface pores, suggesting a remarkable mending effect. In addition, there exists TiO_2 laminae that are deposited on the surface, which acts similarly to the lubricating film. In the contact zone between the work roll and workpiece, the TiO_2 NPs are supposed to play an integrated role of rolling bearings and laminae, which is the primary means to

reduce the friction and hence the rolling force. The mending effect of TiO_2 NPs assists in repairing the surface defects, not only improving the surface finish (see Figures 5 and 6), but also blocking the channels for oxygen penetration. The latter is the other factor that suppresses the growth of oxide scale and meanwhile enhances the surface compactness (see Figures 7 and 10).

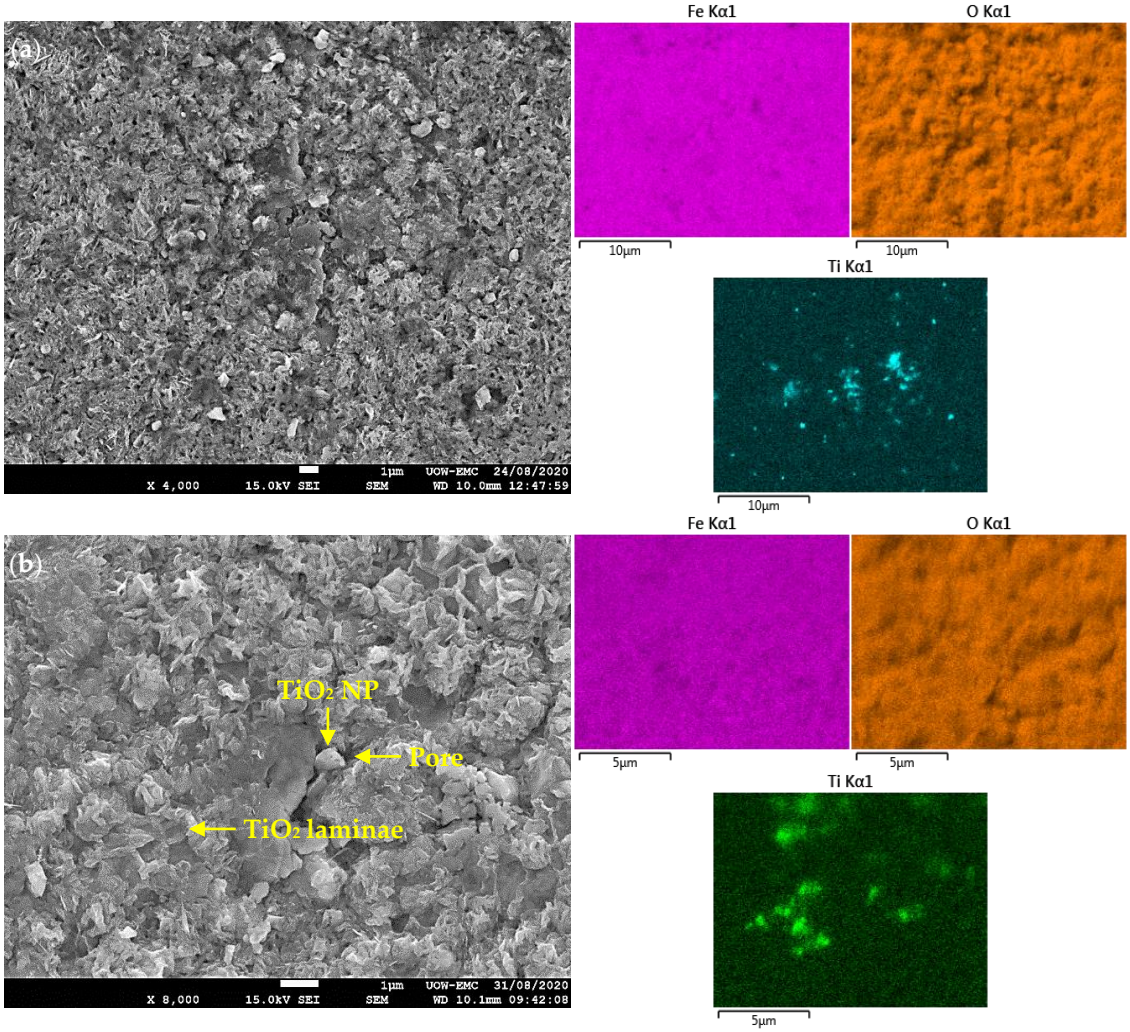

Figure 11. SEM images and energy-dispersive spectrometer (EDS) mappings of the rolled steel surface with lubricant E obtained under the magnifications of (**a**) 4000× and (**b**) 8000×.

Figure 12 shows the SEM image and EDS mappings of the resin/oxide scale interface of the steel rolled with lubricant E. As seen from the SEM image, a thin secondary oxide layer is formed on the top of oxide scale due to the transfer of rolled steel from the runout table to the sealed nitrogen box. Apart from that, TiO_2 NPs can be found along the interface of these two oxide scales according to the EDS mappings of Ti and O. In addition, TiO_2 NPs can also be identified to fill in the defects that exist in the cross section of oxide scale. These findings provide further evidence to support the functions of TiO_2 NPs as discussed in Figure 11.

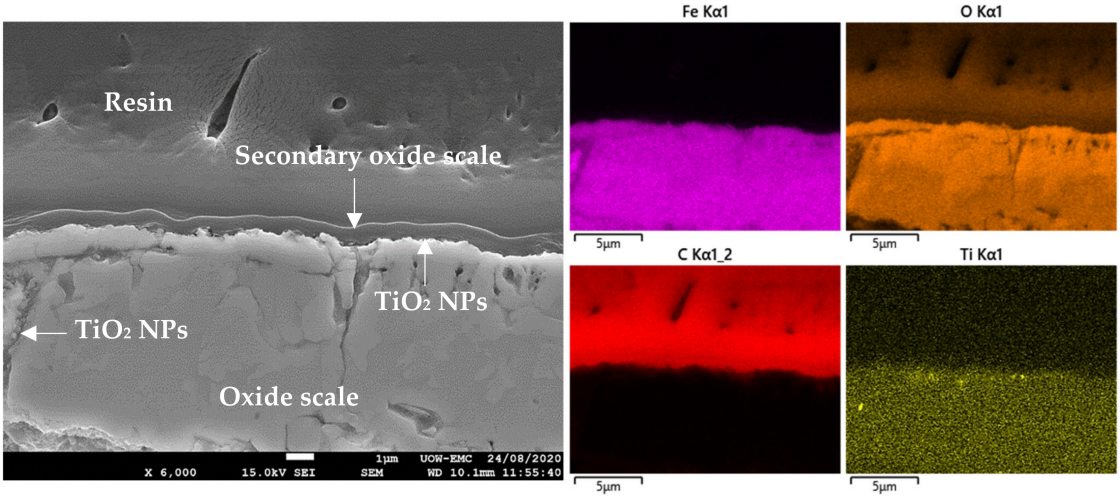

Figure 12. SEM image and EDS mappings of the resin/oxide scale interface of the steel rolled with lubricant E.

4.3. Lubrication Mechanisms

On the basis of the above analyses, the lubrication mechanisms of water-based nanolubricants during hot steel rolling are illustrated in Figure 13. The nanolubricants with excellent wettability on work roll surfaces provide an essential precondition for attaining superior lubrication performance. When the work rolls contacted the hot workpiece, although the nanolubricants suffered an instant loss to some extent at such a high rolling temperature of 850 °C, retained nanolubricants still behaved in the contact zone. Relatively coarse TiO_2 NPs acted as ball bearings and laminae, both of which were committed to decreasing the friction between the work roll and the workpiece. The rolling force would thus be decreased, and this decrease tended to be increasingly significant with enhancing the wettability of lubricant on the work roll surfaces. In the meantime, the TiO_2 NPs were capable of mending the surface defects (pores and cracks), thereby demonstrating relatively small surface roughness after rolling. Last but not least, this mending effect was one of the most important factors that inhibited the propagation of those surface defects and therefore the growth of oxide scale. In another case, the increase in thermal conductivity of the nanolubricants promoted the transformation from austenite to pearlite, generating an increase in surface hardness.

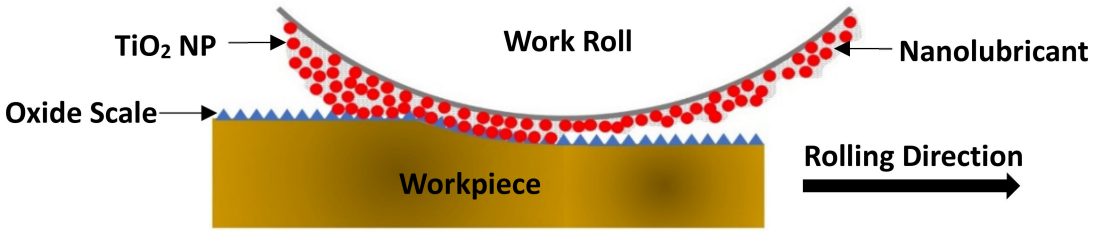

Figure 13. Schematic illustration of lubrication mechanisms using water-based nanolubricants containing TiO_2 NPs during hot steel rolling.

5. Conclusions

In this study, hot steel rolling tests were carried out at 850 °C under pure water and various water-based nanolubricants containing relatively coarse TiO_2 NPs. The lubrication effects of the nanolubricants on rolling force, surface roughness, surface microstructure and hardness, and oxide scale thickness were systematically evaluated, and corresponding lubrication mechanisms were proposed. The main conclusions can be drawn as follows.

(1) The as-synthesised eco-friendly water-based nanolubricants presented excellent dispersion stability, wettability and thermal conductivity.
(2) The rolling force, surface roughness, and oxide scale thickness obtained under pure water condition would be decreased by up to 8.1%, 53.7% and 50%, respectively, by the use of the optimal nanolubricant (4 wt % TiO_2 + 10 wt % glycerol + 0.2 wt % SDBS + 1 wt % Snailcool).
(3) The use of the optimal nanolubricant tended to increase the surface hardness by 4.4%, compared to that of pure water.
(4) The lubrication mechanisms of water-based nanolubricants were ascribed to the synergistic effect of ball bearing, laminae and mending of nano-TiO_2.
(5) The eco-friendly water-based nanolubricants can be obtained using much lower cost additives via a simpler synthesis process, compared to other eco-friendly lubricants.
(6) The optimal water-based nanolubricant will be a promising candidate that can be used in industrial-scale hot steel rolling.

Author Contributions: H.W. performed the experiments in addition to analysing the data and writing the paper; H.K. contributed to the SEM operation; M.H. contributed to the assistance with hot rolling test and the proofreading of the paper. F.L. contributed to the XRD test; S.H. contributed to the provision of additives in the lubricants. Z.X. contributed to the preparation of steel samples; S.J., H.H. and Z.J. contributed to the experimental design and result analysis. All authors have read and agreed to the published version of the manuscript.

Funding: This research was funded by Baosteel-Australia Joint Research and Development Centre (No. BA17004) and Australian Research Council (No. LP150100591).

Acknowledgments: The authors acknowledge the financial support from Baosteel-Australia Joint Research and Development Centre (BAJC) under project of BA17004 and Australian Research Council (ARC) under Linkage Project Program (LP150100591). The authors are grateful to Stuart Rodd, Nathan Hodges, Matthew Franklin and Alex Gonzalez in the workshop of SMART Infrastructure Facility at the University of Wollongong (UOW) for their great support on sample machining and preparation. We would like to extend special thanks to Jun Chen and Yuetong Zhou at UOW for their kind assistance with the measurement of thermal conductivity. We also appreciate Klaudia Wagner at UOW for her guidance on the wettability test. Finally, we wish to acknowledge the Australian National Fabrication Facility (ANFF)-Materials Node for facility access.

Conflicts of Interest: The authors declare no conflict of interest.

References

1. Zhao, J.; Jiang, Z. Thermomechanical processing of advanced high strength steels. *Prog. Mater. Sci.* **2018**, *94*, 174–242. [CrossRef]
2. Jiang, Z.; Tang, J.; Sun, W.; Tieu, A.; Wei, D. Analysis of tribological feature of the oxide scale in hot strip rolling. *Tribol. Int.* **2010**, *43*, 1339–1345. [CrossRef]
3. Matsubara, Y.; Hiruta, T.; Kimura, Y. Effect of Oil Film Thickness on Lubrication Property in Hot Rolling. *ISIJ Int.* **2015**, *55*, 632–636. [CrossRef]
4. Azushima, A.; Xue, W.; Yoshida, Y. Influence of Lubricant Factors on Coefficient of Friction and Clarification of Lubrication Mechanism in Hot Rolling. *ISIJ Int.* **2009**, *49*, 868–873. [CrossRef]
5. Shirizly, A.; Lenard, J.G. The effect of lubrication on mill loads during hot rolling of low carbon steel strips. *J. Mater. Process. Technol.* **2000**, *97*, 61–68. [CrossRef]
6. Xia, W.; Zhao, J.; Wu, H.; Zhao, X.; Zhang, X.; Xu, J.; Jiao, S.; Wang, X.; Zhou, C.; Jiang, Z. Effects of oil-in-water based nanolubricant containing TiO_2 nanoparticles in hot rolling of 304 stainless steel. *J. Mater. Process. Technol.* **2018**, *262*, 149–156. [CrossRef]
7. Li, Y.-L.; Cao, J.-G.; Kong, N.; Wen, D.; Ma, H.-H.; Zhou, Y.-S. The effects of lubrication on profile and flatness control during ASR hot strip rolling. *Int. J. Adv. Manuf. Technol.* **2017**, *91*, 2725–2732. [CrossRef]
8. Matsuoka, S.; Morita, M.; Furukimi, O.; Obara, T. Recrystallization and Related Phenomena. Effect of Lubrication Condition on Recrystallization Texture of Ultra-low C Sheet Steel Hot-rolled in Ferrite Region. *ISIJ Int.* **1998**, *38*, 633–639. [CrossRef]
9. Barrett, C. Influence of lubrication on through thickness texture of ferritically hot rolled interstitial free steel. *Ironmak. Steelmak.* **1999**, *26*, 393–397. [CrossRef]

10. Etou, M.; Fukushima, S.; Sasaki, T.; Haraguchi, Y.; Miyata, K.; Wakita, M.; Tomida, T.; Imai, N.; Yoshida, M.; Okada, Y. Super Short Interval Multi-pass Rolling Process for Ultrafine-grained Hot Strip. *ISIJ Int.* **2008**, *48*, 1142–1147. [CrossRef]
11. Wen, P.; Lei, Y.; Li, W.; Fan, M. Synergy between Covalent Organic Frameworks and Surfactants to Promote Water-Based Lubrication and Corrosion Resistance. *ACS Appl. Nano Mater.* **2020**, *3*, 1400–1411. [CrossRef]
12. Su, F.; Chen, G.; Huang, P. Lubricating performances of graphene oxide and onion-like carbon as water-based lubricant additives for smooth and sand-blasted steel discs. *Friction* **2020**, *8*, 47–57. [CrossRef]
13. Chen, W.; Amann, T.; Kailer, A.; Rühe, J. Macroscopic Friction Studies of Alkylglucopyranosides as Additives for Water-Based Lubricants. *Lubricants* **2020**, *8*, 11. [CrossRef]
14. He, A.; Huang, S.; Yun, J.-H.; Jiang, Z.; Stokes, J.R.; Jiao, S.; Wang, L.; Huang, H. Tribological Characteristics of Aqueous Graphene Oxide, Graphitic Carbon Nitride, and Their Mixed Suspensions. *Tribol. Lett.* **2018**, *66*, 42. [CrossRef]
15. He, A.; Huang, S.; Yun, J.-H.; Jiang, Z.; Stokes, J.R.; Jiao, S.; Wang, L.; Huang, H. The pH-dependent structural and tribological behaviour of aqueous graphene oxide suspensions. *Tribol. Int.* **2017**, *116*, 460–469. [CrossRef]
16. Huo, M.; Wu, H.; Xie, H.; Zhao, J.; Su, G.; Jia, F.; Li, Z.; Lin, F.; Li, S.; Zhang, H.; et al. Understanding the role of water-based nanolubricants in micro flexible rolling of aluminium. *Tribol. Int.* **2020**, *151*, 106378. [CrossRef]
17. He, J.; Sun, J.; Meng, Y.; Pei, Y. Superior lubrication performance of MoS2-Al2O3 composite nanofluid in strips hot rolling. *J. Manuf. Process.* **2020**, *57*, 312–323. [CrossRef]
18. Meng, Y.; Sun, J.; Wu, P.; Dong, C.; Yan, X. The Role of Nano-TiO_2 Lubricating Fluid on the Hot Rolled Surface and Metallographic Structure of SS41 Steel. *Nanomaterials* **2018**, *8*, 111. [CrossRef]
19. Bao, Y.; Sun, J.; Kong, L. Effects of nano-SiO_2 as water-based lubricant additive on surface qualities of strips after hot rolling. *Tribol. Int.* **2017**, *114*, 257–263. [CrossRef]
20. Kong, L.; Sun, J.; Bao, Y.; Meng, Y. Effect of TiO_2 nanoparticles on wettability and tribological performance of aqueous suspension. *Wear* **2017**, *376-377*, 786–791. [CrossRef]
21. Rahman, M.M.; Rahman, M.M. Experimental investigation of flank wear in end milling of aluminum alloy with water-based TiO_2 nanofluid lubricant in minimum quantity lubrication technique. *Int. J. Adv. Manuf. Technol.* **2016**, *86*, 2527–2537. [CrossRef]
22. Ohenoja, K.; Saari, J.; Illikainen, M.; Niinimäki, J. Effect of molecular weight of sodium polyacrylates on the particle size distribution and stability of a TiO_2 suspension in aqueous stirred media milling. *Powder Technol.* **2014**, *262*, 188–193. [CrossRef]
23. Gu, Y.; Zhao, X.; Liu, Y.; Lv, Y. Preparation and Tribological Properties of Dual-Coated TiO_2 Nanoparticles as Water-Based Lubricant Additives. *J. Nanomater.* **2014**, *2014*, 2. [CrossRef]
24. Wu, H.; Jia, F.; Zhao, J.; Huang, S.; Wang, L.; Jiao, S.; Huang, H.; Jiang, Z. Effect of water-based nanolubricant containing nano-TiO_2 on friction and wear behaviour of chrome steel at ambient and elevated temperatures. *Wear* **2019**, *426*, 792–804. [CrossRef]
25. Wu, H.; Zhao, J.; Cheng, X.; Xia, W.; He, A.; Yun, J.-H.; Huang, S.; Wang, L.; Huang, H.; Jiao, S.; et al. Friction and wear characteristics of TiO_2 nano-additive water-based lubricant on ferritic stainless steel. *Tribol. Int.* **2018**, *117*, 24–38. [CrossRef]
26. Wu, H.; Zhao, J.; Xia, W.; Cheng, X.; He, A.; Yun, J.-H.; Wang, L.; Huang, H.; Jiao, S.; Huang, L.; et al. A study of the tribological behaviour of TiO_2 nano-additive water-based lubricants. *Tribol. Int.* **2017**, *109*, 398–408. [CrossRef]
27. Wu, H.; Zhao, J.; Xia, W.; Cheng, X.; He, A.; Yun, J.H.; Wang, L.; Huang, H.; Jiao, S.; Huang, L.; et al. Analysis of TiO_2 nano-additive water-based lubricants in hot rolling of microalloyed steel. *J. Manuf. Process.* **2017**, *27*, 26–36. [CrossRef]
28. Wu, H.; Zhao, J.; Luo, L.; Huang, S.; Wang, L.; Zhang, S.; Jiao, S.; Huang, H.; Jiang, Z. Performance Evaluation and Lubrication Mechanism of Water-Based Nanolubricants Containing Nano-TiO_2 in Hot Steel Rolling. *Lubricants* **2018**, *6*, 57. [CrossRef]
29. Wu, H.; Jiang, C.; Zhang, J.; Huang, S.; Wang, L.; Jiao, S.; Huang, H.; Jiang, Z. Oxidation Behaviour of Steel During hot Rolling by Using TiO_2-Containing Water-Based Nanolubricant. *Oxid. Met.* **2019**, *92*, 315–335. [CrossRef]

30. Wu, H.; Jia, F.; Li, Z.; Lin, F.; Huo, M.; Huang, S.; Sayyar, S.; Jiao, S.; Huang, H.; Jiang, Z. Novel water-based nanolubricant with superior tribological performance in hot steel rolling. *Int. J. Extreme Manuf.* **2020**, *2*, 025002. [CrossRef]
31. Hanaor, D.; Assadi, M.H.N.; Li, S.; Yu, A.; Sorrell, C.C. Ab initio study of phase stability in doped TiO_2. *Comput. Mech.* **2012**, *50*, 185–194. [CrossRef]
32. Greenwood, N.N.; Earnshaw, A. *Chemistry of the Elements*; Elsevier: Amsterdam, The Netherlands, 2012.
33. Xia, W.; Zhao, J.; Wu, H.; Zhao, X.; Zhang, X.; Xu, J.; Hee, A.C.; Jiang, Z. Effects of Nano-TiO_2 Additive in Oil-in-Water Lubricant on Contact Angle and Antiscratch Behavior. *Tribol. Trans.* **2017**, *60*, 362–372. [CrossRef]
34. Anderson, W. Wettability Literature Survey—Part 2: Wettability Measurement. *J. Pet. Technol.* **1986**, *38*, 1246–1262. [CrossRef]
35. Özerinç, S.; Kakaç, S.; Yazıcıoğlu, A.G. Enhanced thermal conductivity of nanofluids: A state-of-the-art review. *Microfluid. Nanofluidics* **2010**, *8*, 145–170. [CrossRef]
36. Cannio, M.; Ponzoni, C.; Gualtieri, A.F.; Lugli, E.; Leonelli, C.; Romagnoli, M. Stabilization and thermal conductivity of aqueous magnetite nanofluid from continuous flows hydrothermal microwave synthesis. *Mater. Lett.* **2016**, *173*, 195–198. [CrossRef]
37. Kedzierski, M.; Brignoli, R.; Quine, K.; Brown, J. Viscosity, density, and thermal conductivity of aluminum oxide and zinc oxide nanolubricants. *Int. J. Refrig.* **2017**, *74*, 3–11. [CrossRef] [PubMed]
38. Warrier, P.; Teja, A. Effect of particle size on the thermal conductivity of nanofluids containing metallic nanoparticles. *Nanoscale Res. Lett.* **2011**, *6*, 247. [CrossRef]
39. Tadjarodi, A.; Zabihi, F. Thermal conductivity studies of novel nanofluids based on metallic silver decorated mesoporous silica nanoparticles. *Mater. Res. Bull.* **2013**, *48*, 4150–4156. [CrossRef]
40. Mishra, S.; Nayak, M.; Misra, A. Thermal Conductivity of Nanofluids-A Comprehensive Review. *Int. J. Thermofluid Sci. Technol.* **2020**, *7*, 7. [CrossRef]
41. Mukherjee, S.; Mishra, P.C.; Chaudhuri, P. Enhancing Thermo-Economic Performance of TiO_2-Water Nanofluids: An Experimental Investigation. *JOM* **2020**, 1–10. [CrossRef]
42. Wu, Y.-X.; Fu, J.-X.; Zhang, H.; Xu, J.; Zhai, Q. Effects of Rolling and Cooling Conditions on Microstructure of Umbrella-Bone Steel. *High Temp. Mater. Process.* **2017**, *36*, 947–953. [CrossRef]
43. Basabe, V.V.; Szpunar, J.A. Growth Rate and Phase Composition of Oxide Scales during Hot Rolling of Low Carbon Steel. *ISIJ Int.* **2004**, *44*, 1554–1559. [CrossRef]
44. Chen, R. Review of the High-Temperature Oxidation of Iron and Carbon Steels in Air or Oxygen. *Oxid. Met.* **2003**, *59*, 433–468. [CrossRef]
45. Hayashi, S.; Mizumoto, K.; Yoneda, S.; Kondo, Y.; Tanei, H.; Ukai, S. The Mechanism of Phase Transformation in Thermally-Grown FeO Scale Formed on Pure-Fe in Air. *Oxid. Met.* **2014**, *81*, 357–371. [CrossRef]